

1 Chromatographic retention behaviour, modelling and optimization of a UHPLC-UV  
2 separation of the regioisomers of the Novel Psychoactive Substance (NPS) methoxphenidine  
3 (MXP)

4

5 Bernard O. Boateng<sup>a</sup>, Mark Fever<sup>b</sup>, Darren Edwards<sup>a,d</sup>, Patrik Petersson<sup>c</sup>, Melvin R.  
6 Euerby<sup>a,b,e,\*</sup> and Oliver B. Sutcliffe<sup>f,\*</sup>

7

8 <sup>a</sup> Strathclyde Institute of Pharmacy and Biomedical Sciences, University of Strathclyde, 161  
9 Cathedral Street, Glasgow, G4 0RE, UK.

10 <sup>b</sup> Hichrom Ltd, 1 The Markham Centre, Station Road, Theale, Reading Berkshire, RG7 4PE,  
11 UK.

12 <sup>c</sup> Novo Nordisk A/S, Novo Nordisk Park, DK-2760 Måløv, Denmark.

13 <sup>d</sup> Present address: Drug Discovery Unit, School of Life Sciences, Sir James Black Centre,  
14 University of Dundee, Dow Street, Dundee DD1 5EH, Scotland, UK.

15 <sup>e</sup> Present address: Shimadzu UK Limited, Mill Court, Featherstone Road, Wolverton Mill  
16 South, Milton Keynes, MK12 5RD, UK.

17 <sup>f</sup> MANchester DRug Analysis and Knowledge Exchange (MANDRAKE), School of Science and  
18 the Environment, Faculty of Science and Engineering, Manchester Metropolitan University,  
19 John Dalton Building, Chester Street, Manchester, M1 5GD, UK.

20

21 \* corresponding authors, [melvin.euerby@strath.ac.uk](mailto:melvin.euerby@strath.ac.uk) and [o.sutcliffe@mmu.ac.uk](mailto:o.sutcliffe@mmu.ac.uk)

22

23 Abstract

24 A detailed investigation into the chromatographic retention behaviour and separation of the  
25 three regioisomers of the Novel Psychoactive Substance (NPS) methoxphenidine (i.e. 2-, 3-  
26 and 4-MXP isomers) has revealed the ionization state of the analyte and stationary phase, to  
27 be the controlling factor in dictating which retention mechanism is in operation. At low pH,  
28 poor separation and retention was observed. In contrast, at intermediate pH, enhanced  
29 retention and separation of the three MXP isomers was obtained; it appeared that there  
30 was a synergistic effect between the electrostatic and hydrophobic mechanisms. At high  
31 pH, the MXP isomers were retained by hydrophobic retention. Accurate retention time  
32 predictions (<0.5%) were achievable using non-linear retention models (3 x 3). This allowed  
33 the optimization of the gradient separation of the MXP isomers using a two-dimensional  
34 gradient and temperature design space. Prediction errors for peak width and resolution  
35 were, in most cases, lower than 5%. The use of linear models (2 x 2) still afforded retention  
36 time and resolution accuracies of < 2.3 and 11% respectively. A rapid and highly sensitive LC-  
37 MS friendly method (i.e.  $R_{s \text{ min}} > 3$  within 2.5 minutes) was predicted and verified. The

38 developed methodology should be highly suitable for the rapid, specific and sensitive  
39 detection and control of MXP regioisomers.

40

41 Keywords

- 42 • Reversed phase HPLC
- 43 • Two-dimensional retention modelling
- 44 • Regioisomeric methoxyphenidines
- 45 • Novel Psychoactive Substance
- 46 • Chromatographic optimization
- 47 • Retention mechanisms

48

49 1 Introduction

50 Designer drugs are analogues of controlled substances that are designed to produce effects  
51 similar to the controlled substances they mimic<sup>2</sup> [1]. The rate at which such substances are  
52 appearing poses significant issues for forensic laboratories with respect to identification and  
53 quantification, as validated analytical methods and reference standards are not usually  
54 available [4].

55 Dissociative diarylethylamine anaesthetics (Figure 1) such as diphenidine (1) [5] and 2-  
56 methoxyphenidine (2-MXP, 2) [6] are substances that distort perceptions, produce feelings of  
57 detachment and induce a state of anaesthesia by antagonising ionotropic *N*-methyl-*D*-  
58 aspartate receptors (NMDAR) in the central nervous system [7]. Though both the supply and  
59 production of diphenidine and 2-methoxyphenidine is now controlled in the United Kingdom  
60 by the Psychoactive Substances Act (2016) [8], the global prevalence of novel  
61 diarylethylamine derivatives still raises considerable legal and analytical challenges in the  
62 forensic identification of these materials. 2-MXP has been implicated in a number of  
63 fatalities in Europe [9, 10] and is encountered in both tablet and powder forms. Recently,  
64 the reversed-phase liquid chromatographic (RP-LC) separation of the regioisomers of  
65 methoxyphenidine (2-MXP, 2; 3-MXP, 3 and 4-MXP, 4, see Figure 1) has been reported using  
66 a superficially porous phenyl hexyl material (i.e. 2.6 µm Kinetex) coupled with a shallow  
67 MeCN / formic acid gradient at 30 °C (i.e. 0.25% MeCN/min). While the 2-isomer was well  
68 resolved from the other two isomers, only partial separation of the 3- and 4-isomers was  
69 observed (the elution order was reported to be 3-MXP, 4-MXP, 2-MXP isomer). However,  
70 the paper [6] did not prove evidence of any systematic investigation into the retention  
71 behaviour. Analytical differentiation of regioisomers is a significant issue in forensic drug  
72 analysis, because, in most cases, legal controls are placed on only one or two of the  
73 conceivable isomers and require a forensic scientist to show unequivocally that a sample  
74 submitted is in fact a controlled drug and not one of the non-controlled regioisomers. This  
75 can be readily achieved using Nuclear Magnetic Resonance (NMR) spectroscopy, however,  
76 few forensic laboratories have such instruments and the discrimination of regioisomers  
77 using the technique is both cost and labour intensive. Geyer *et al.* has recently published a

78 validated GC-(EI)-MS protocol for the qualitative and quantitative analysis of thirteen  
79 diarylethylamine derivatives (including 2-MXP and its isomers) in seized powder samples –  
80 however, the published method has significant limitations in terms of overall analysis time  
81 (*circa.* 45 mins) [11]. This HPLC method provides, for the first time, both a general screening  
82 method and quantification of the active components for seized solid samples of  
83 methoxphenidine, which is significantly superior to the previously reported GC-MS [11] and  
84 HPLC [6, 10] methods in terms of overall run time (7 mins) and resolution of the  
85 regioisomers.

86 In contrast, this current paper reports the retention behaviour and separation of the three  
87 regioisomeric methoxphenidines as a function of pH, temperature, proportion of organic  
88 modifier and buffer concentration on a variety of RP columns of widely differing  
89 chromatographic selectivity. Six new generation RP silica phases were selected from the  
90 same manufacturer in order to minimize any problems associated with differing base silica  
91 acidities [12]. Three totally porous particles (TPP) (i.e. C18-AR, C18 and C18-PFP) were  
92 selected as previously these stationary phases have demonstrated complementary  
93 chromatographic selectivity to each other [12]. In addition, three high pH stable phases  
94 (which have been shown to possess similar selectivity to their non-high pH stable TPP  
95 counterparts [i.e. TPP C18 versus the TPP and superficially porous particles (SPP) SuperC18  
96 materials plus the TPP C18-AR and SPP Super Phenyl hexyl phases] were additionally  
97 selected in order to allow the basic MXP regioisomers to be chromatographed, at high pH, in  
98 their ion-suppressed form. The three-high pH stable phases have been reported to show  
99 good stability up to pH 11 [13].

100 A detailed investigation into the retention mechanism of these regioisomeric substances  
101 was performed as a function of stationary phase chemistry, mobile phase pH, proportion of  
102 organic modifier and buffer concentration. The most promising chromatographic conditions  
103 were then subjected to retention modelling and optimization in order to develop a rapid,  
104 highly selective and robust UHPLC-UV separation of the 2-, 3- and 4-MXP isomers, within  
105 bulk forensic samples, using LC-MS friendly conditions.

106

## 107 2 Materials and methods

### 108 2.1 Chemicals and Reagents

109 All water and solvents used were HPLC grade, test analytes and mobile phase chemicals  
110 were supplied by Sigma-Aldrich (Poole, UK) and Fisher Scientific (Loughborough, UK).  
111 Samples of the three methoxphenidine isomers (2 – 4) were prepared, under UK [Home  
112 Office] Drug Licence (No. 337201), as their corresponding hydrochloride salts at Manchester  
113 Metropolitan University. The synthesis of the racemic target compounds was achieved using  
114 the previously reported method [11] in 52 – 77% overall yield. The hydrochloride salts were  
115 obtained as stable, colourless to off-white powders (Figure 1) and determined to be soluble  
116 ( $10 \text{ mg mL}^{-1}$ ) in deionised water, methanol, dichloromethane and dimethylsulfoxide. To  
117 ensure the authenticity of the materials utilized in this study the three synthesized samples

118 were fully structurally characterized by <sup>1</sup>H-NMR, <sup>13</sup>C-NMR, GC-MS and ATR-FTIR and the  
119 purity of all samples confirmed by elemental analysis (>99.5% in all cases) [11].

120

### 121 2.1.1 Methoxphenidine (MXP) isomers

122 Stock solutions of the individual isomers of methoxphenidine were made up in MeCN/water  
123 (1:1 v/v) at a concentration of 1 mg mL<sup>-1</sup>. A mixture of the isomers was prepared and then  
124 diluted to 100 µg mL<sup>-1</sup> (of each isomer) with MeCN/water (1:1 v/v) for the chromatographic  
125 studies.

126

## 127 2.2 Software

128 LogD and *pK<sub>a</sub>* values were predicted (ACD/Percepta, Toronto, Canada, version 2016.1.1) and  
129 retention modelling and optimization (ACD/LC Simulator, version 2016.1.1) were performed  
130 using software from ACD/Labs (Advanced Chemistry Development Inc., Toronto, Canada).  
131 Buffers of a desired pH and buffer concentration were determined by the Buffer Maker  
132 software (ChemBuddy, Marki, Poland, version 1.0.1.55).

133

## 134 2.3 Instrumentation

### 135 2.3.1 UHPLC instrumentation

136 UHPLC was performed on the following instrumentation: Agilent 1290 Infinity UHPLC  
137 systems (Agilent Technologies, Waldbronn, Germany) equipped with either binary (model  
138 G4220A) or quaternary (model G4204A) pumps used in conjunction with an integrated  
139 degasser (model G4220A), autosampler (model G4226A), column oven model (G1316C),  
140 photodiode array detector (model G4212A) equipped with a 1 µL / 10 mm pathlength flow  
141 cell, 380 µL Jet Weaver mixer and a 12 position / 13 port solvent selection valve (model  
142 G1160A), was used to allow the automated selection of up to 12 different eluents from  
143 mobile phase line C of the Agilent 1290 Infinity quaternary UHPLC, the system(s) was  
144 controlled and data collected by means of ChemStation (Agilent Technologies, Waldbronn,  
145 Germany, version B.04.03). Shimadzu Nexera X2 UHPLC (Shimadzu UK Ltd, Milton Keynes,  
146 UK) equipped with LC-30AD pumps, DGU-20A5R degassers, SIL-30AC autosampler, CTO-  
147 20AC column oven, SPD-M30A photodiode array detector equipped with a 10 µL / 10 mm  
148 pathlength flow cell, 180 µL mixer, the system was controlled and data collected by means  
149 of LabSolutions software (Shimadzu UK Ltd, Milton Keynes, UK, version 5.86).

150

## 151 2.4 Liquid Chromatography

152 pH measurements were recorded in the aqueous fraction of the mobile phase and quoted  
153 as <sup>w</sup>pH. At least 20 column volumes of the appropriate mobile phase were flushed  
154 through the columns prior to commencing the testing or on changing the mobile phase

155 conditions. The totally porous ACE C18, C18-PFP, C18-AR (5  $\mu\text{m}$ , 100 $\text{\AA}$ , 150 x 4.6 mm I.D.  
156 format), C18-AR, SuperC18 (3  $\mu\text{m}$ , 100 $\text{\AA}$ , 50 x 4.6 mm I.D. format), ACE UltraCore  
157 superficially porous SuperC18 and SuperPhenylhexyl (2.5  $\mu\text{m}$ , 100 $\text{\AA}$ , 50 x 4.6 mm I.D.  
158 format) columns were as supplied by Advanced Chromatography Technologies (Aberdeen,  
159 Scotland, UK). The integrity of all the columns was confirmed periodically throughout the  
160 experiments by injecting a suitable non-polar test mixture (i.e. uracil, toluene, biphenyl,  
161 dimethyl phthalate and phenanthrene) before and after the experiments. All columns gave  
162 retention times, efficiency and peak symmetry levels >95% of their initial value. The mobile  
163 phase was degassed and mixed on-line for the aqueous / organic mixtures.

164 The first baseline disturbance for a water injection was used as the dead time ( $t_M$ ) marker.  
165 A flow rate of 1.0 mL min<sup>-1</sup> and a 2  $\mu\text{L}$  injection was used in all experiments and a column  
166 temperature was maintained between 20 – 70  $^{\circ}\text{C}$ . The diode array detector was set to  
167 monitor a wavelength of 278 nm with a reference at 360 nm. The data sampling rate was  
168 set at 40 Hz. Peak width and symmetry was determined at half height as reported by the  
169 ChemStation software or LabSolutions software. For the retention modelling the peak  
170 width at base was calculated by multiplying the peak width at half height by 1.699 [to  
171 generate the 4 $\sigma$ , United States Pharmacopeia (USP) peak width values]. Chromatographic  
172 values reported are the average of duplicate injections. Retention factors ( $k$ ) were  
173 calculated for isocratic conditions using the following equation;  $k = (t_R - t_M) / t_M$ . Where  $t_R$  =  
174 retention time of the isomer and  $t_M$  = void time of an unretained analyte.

175

176 2.4.1 Effect of ammonium acetate concentration on the retention of the MXP isomers (see  
177 section 3.3)

178 Evaluation of the effect of ammonium acetate (pH 6.8) concentration (1 – 14 mM) on the  
179 retention of the methoxphenidine isomers was performed on an ACE C18-AR 3  $\mu\text{m}$  50 x 4.6  
180 mm column at 54 % MeCN concentration, 30  $^{\circ}\text{C}$ , 1 mL min<sup>-1</sup> using the Agilent 1290 Infinity  
181 Quaternary UHPLC. Mobile phase A) 100 mM ammonium acetate (pH 6.8 unadjusted), B)  
182 MeCN, C) water. The appropriate buffer concentrates were mixed on-line, for example 10  
183 mM buffer in MeCN/water was prepared by mixing A:B:C in the ratio 10:54:36 v/v/v.

184

185 2.4.2 Effect of the proportion of acetonitrile (MeCN) on the retention of the MXP isomers  
186 (see section 3.4)

187 Evaluation of the effect of the proportion of MeCN (18 – 63 % v/v) on the retention of the  
188 methoxphenidine isomers was performed on an ACE C18-AR and ACE SuperC18, 3  $\mu\text{m}$ , 50 x  
189 4.6 mm column, 1 mL min<sup>-1</sup>, 60  $^{\circ}\text{C}$ , mobile phase A) 10 mM ammonium acetate (pH 6.8  
190 unadjusted), 10 mM ammonium formate (pH 3) or 18.6 mM ammonia (pH 10.7) in water, B)  
191 the appropriate buffer in MeCN/water (9:1 v/v) using the Agilent 1290 Infinity Binary  
192 UHPLC.

193

194 2.4.3 Effect of temperature on the retention of the MXP isomers (see section 3.5)

195 Evaluation of the effect of temperature (20 -70 °C) on the retention of the methoxphenidine  
196 isomers was performed on an ACE C18-AR, 3 µm, 50 x 4.6 mm column using 60 %B (i.e. 54 %  
197 v/v MeCN), 1 mL min<sup>-1</sup>, mobile phase A) 10 mM ammonium acetate (pH 6.8 unadjusted) in  
198 water, B) 10 mM ammonium acetate (pH of 6.8 unadjusted) in MeCN/water (9:1 v/v) using  
199 the Shimadzu Nexera X2 UHPLC.

200

201 2.4.4 Effect of pH on the retention of the MXP isomers (see section 3.2)

202 Evaluation of the effect of pH on the retention of the methoxphenidine isomers was  
203 performed on ACE UltraCore SuperC18 and C18-AR columns, 2.5 and 3 µm respectively, 50 x  
204 4.6 mm column at 60 %B (i.e. 54 % v/v MeCN), 50 °C, 1 mL min<sup>-1</sup>, mobile phase A) 10 mM  
205 ammonium formate pH 3, B) 10 mM ammonium acetate (unadjusted pH of 6.8) and c) 18  
206 mM ammonia (unadjusted pH of 10.7) using the Agilent 1290 Infinity Quaternary UHPLC.

207

208 2.4.5 Effect of pH over the range pH 8 -10.7 on the retention of the MXP isomers (see  
209 section 3.2.3)

210 Evaluation of the effect of high pH (pH 8, 9, 9.25, 9.5, 9.75, 10 and 10.7) on the retention of  
211 the methoxphenidine isomers was performed on an ACE Ultracore SuperC18, 2.5 µm, 50 x  
212 4.6 mm column using 10 mM ammonia / acetic acid buffers (ammonia concentration kept  
213 constant) in MeCN/water (54:46 v/v), 50 °C, 1 mL min<sup>-1</sup> using the Agilent 1290 Infinity  
214 Quaternary UHPLC. Stock pH buffers were prepared as described by the Buffer Maker  
215 Software.

216

217 2.5 Retention modelling

218

219 2.5.1 Two-dimensional retention modelling and optimization: Gradient time *versus*  
220 temperature on the C18-AR at pH 6.8 (see section 3.7.2)

221 An ACE C18-AR column (3 µm, 50 x 4.6 mm) was used at a flow rate of 1 mL min<sup>-1</sup> using the  
222 Shimadzu Nexera X2 UHPLC. Sixteen input runs and six validation runs were performed  
223 (see section 3.7.2, Figure 6). Mobile phase A consisted of 10 mM ammonium acetate  
224 (unadjusted pH 6.8) and mobile phase B of 10 mM ammonium acetate (unadjusted pH 6.8)  
225 in MeCN/water (9:1 v/v). A temperature range of 30 to 70 °C was investigated (see Figure  
226 6). The %B gradient range was run between 40 and 70 %B. After the selected gradient run  
227 time ( $t_G$ ) was reached, a 5-minute hold time at 70%B, 1-minute ramp down to 40%B, and a  
228 5-minute post time at 40%B were employed.

229

230

231 3 Results and Discussion

232

233 3.1 Chromatographic separation of the methoxphenidine (MXP) regioisomers as a  
234 function of stationary phase chemistry

235 The TPP ACE C18, C18-AR and C18-PFP and the high pH stable SPP SuperC18 and  
236 SuperPhenylhexyl phases, which possess differing bonded ligands on the silica, have  
237 recently been showed to exhibit differing chromatographic selectivities (see Supplementary  
238 electronic information Table SEI 1) due to the ligands' differing propensity to participate in  
239 hydrophobic, aromatic (i.e.  $\pi$  acid and  $\pi$  base interactions), dipole – dipole interactions,  
240 hydrogen bonding and electrostatic interaction with various analytes under a range of  
241 chromatographic conditions [13]. Hence, it was somewhat surprising that these phases  
242 failed to exhibit any major selectivity differences irrespective of mobile phase pH suggesting  
243 that the MXP interactions with the differing stationary phase ligands was not the controlling  
244 retention mechanism.

245

246 3.2 Chromatographic separation of the methoxphenidine (MXP) regioisomers as a  
247 function of pH

248 The regioisomers of methoxphenidine are hydrophobic compounds with tertiary amine  
249 functionality, with calculated  $pK_a$  values of 8.7, 9.1 and 9.4 for the 2-, 3- and 4-MXP isomers  
250 respectively. Hence, the effect of pH was investigated in order to assess the influence of  
251 hydrophobic and electrostatic interactions on their chromatographic retention.

252

253 3.2.1 Chromatographic separation of the methoxphenidine (MXP) regioisomers at low pH

254 Chromatography of the regioisomeric analytes (Figure 1, 2 – 4) on the TPP ACE C18, C18-AR  
255 and C18-PFP, at low pH, resulted in low retention and only partial separation of the isomers  
256 (data not shown). The low retention and the elution order observed on the three TPP  
257 phases, at low pH with 10 mM ammonium formate pH 3 mirrored that was previously  
258 reported by McLaughlin *et al* [6] using another phenylhexyl phase (i.e. the 2-isomer (2)  
259 eluted after the partial separation of the 3- and 4- isomers). Separation selectivity was not  
260 improved even when lower %MeCN containing mobile phases were employed in order to  
261 improve retention (see Figure 4a). The low retention (see Figure 2a for a typical  
262 chromatogram on the SPP SuperC18 column) may be attributed to the mutual repulsion of  
263 the adsorbed protonated MXP isomers and the low acidity of the new generation silica  
264 columns used in this study.

265

266

267 3.2.2 Chromatographic separation of the methoxphenidine (MXP) regioisomers at  
268 intermediate pH

269 Chromatography at pH 6.8 (i.e. 10 mM ammonia acetate) using the C18-AR, SuperC18 and  
270 SuperPhenylHexyl phases resulted in enhanced retention and excellent separation of the  
271 regioisomers (the C18 and C18-PFP phases were not evaluated). Figure 2b is typical of the  
272 separation that could be achieved on these phases at intermediate pH using the SPP  
273 SuperC18. Once again, the same elution order (i.e. 2-MXP, 4-MXP, 3-MXP) was obtained on  
274 each phase, which was surprising, given the large chromatographic selectivity differences  
275 that exists between the C18 and phenyl phases (see Supplementary electronic information  
276 Table SEI 1). The elution order at low and intermediate pH (i.e. 2-MXP, 4-MXP, 3-MXP) was  
277 different to that observed at high pH (i.e. 4-MXP, 3-MXP, 2-MXP see Figures 2a -c).

278

### 279 3.2.3 Chromatographic separation of the methoxphenidine (MXP) regioisomers at high pH

280 Chromatography on the high pH stable SPP & TPP phases (i.e. SuperC18 and  
281 SuperPhenylHexyl) at pH 10.7 (i.e. 18 mM ammonia) exhibited enhanced retention and  
282 good resolution of all of the isomers with the same elution order (i.e. 4-MXP, 3-MXP, 2-  
283 MXP) irrespective of the phase chemistry. Figure 2c highlights a typical separation at high  
284 pH conditions using the SPP SuperC18 phase. Interestingly, the elution order of the isomers  
285 at high pH was different to that observed using intermediate pH conditions (i.e. 2-MXP, 4-  
286 MXP, 3-MXP). It is presumed that the high pH of the mobile phase renders the MXP  
287 molecules uncharged hence eliminating the possibility of ion exchange interactions and  
288 increasing the hydrophobic and  $\pi$ - $\pi$  interaction of the neutral MXP analytes with the  
289 stationary phase. As only small differences in selectivity were observed between the C18  
290 and phenyl phases, we must conclude that there is minimal  $\pi$ - $\pi$  interaction of the analytes  
291 with the phenyl phase, this may be attributed to the fact that MeCN was used as the organic  
292 modifier [14,15].

293 The retention of each of the isomers was in line with their estimated logD values in that  
294 greater retention was observed at pH 10.7 when the MXP isomers were in their unionized  
295 forms. (e.g. the 4-MXP's LogD values were estimated at pH 3, 6.8 and 10.7 to be 1.76, 2.41  
296 and 4.84 respectively).

297 In order to gain a better understanding of the retention behaviour of the MXP isomers at pH  
298 conditions spanning their estimated  $pK_a$  values [i.e. ACD Percepta estimates of 9.4 (4-MXP),  
299 9.1 (3-MXP), and 8.7 (2-MXP)] their retention over the pH range of 8 – 11 was investigated  
300 on the high pH stable SPP SuperC18 at constant ammonia concentration (see  
301 Supplementary electronic information Figure SEI 1). Up to a  $w/w$  pH of 9.5, the elution order  
302 remained the same as that at pH 6.8; the retention of all the isomers becoming  
303 progressively longer presumably due to a greater influence from hydrophobic retention  
304 mechanisms as the mobile phases becomes progressively more alkaline and the MXP  
305 isomers less protonated. Between  $w/w$  pH 9.75 and 11 (the latter is the maximum operating  
306 pH for this phase) a switch in the elution order was observed. The 2-MXP which between  $w/w$   
307 pH 6.8 – 9.5 eluted before the 4-MXP and 3-MXP isomers respectively, at  $w/w$  pH 11 eluted  
308 after the 4-MXP and 3-MXP isomers respectively. The same observations were seen on

309 another high pH stable phase (i.e. the bridged ethyl hybrid - XBridge C18 phase – data not  
310 shown).

311 Addition of sodium chloride into the high pH mobile phase with the TPP SuperC18 phase  
312 (see Supplementary electronic information Figure SEI 2) failed to affect the retention time of  
313 the MXP regioisomers due to the fact that they were chromatographed in their ion-  
314 suppressed form at pH 10.7 (i.e. as the free bases). In comparison, the addition of sodium  
315 chloride to the intermediate pH mobile decreased the retention of the methoxphenidine  
316 isomer as expected due to competition of the positively charged sodium and MXP ions for  
317 the negatively charged silanol groups on the surface of the stationary phase.

318 Due to the enhanced separation (i.e. resolution and speed) of the isomers at intermediate  
319 pH, a more detailed study into the chromatographic parameters which control their  
320 retention was performed at intermediate pH using the ACE C18-AR and SuperC18 phases as  
321 phase chemistry did not appear to be a major factor in determining chromatographic  
322 selectivity.

323

### 324 3.3 Effect of buffer concentration at intermediate pH

325 The effect of ammonium acetate concentration was investigated at 30 °C with a  $w_w$  pH 6.8  
326 mobile phase on the C18-AR phase (see Figure 3). According to ion exchange theory [16-18]  
327 retention has been proposed to be related to buffer concentration as expressed in Equation  
328 1.

329

$$330 \log k = a + b \log x \quad \text{Equation 1}$$

331

332 where  $k$  = retention factor,  $a$ ,  $b$  and  $c$  are coefficients and  $x$  = chromatographic variable (i.e.  
333 proportion of organic or buffer concentration)

334

335 Equation 1 did not provide a good fit for the data shown in Figure 3 so a more complex  
336 model, as described by Equation 2, was employed.

337

$$338 \log k = a + b \log x + c (\log x)^2 \quad \text{Equation 2}$$

339

340 The observation that increased buffer concentrations generated reduced retention of the  
341 MXP isomers highlighted that there is an ion exchange mechanism contributing to retention  
342 at intermediate pH.

343

344

345 3.4 Effect of the proportion of MeCN at intermediate pH

346 In contrast to the expected linear relationship (see Equation 3) between the  $\log k$  of the  
347 MXP isomers and the proportion of MeCN in the mobile phase [19, 20], a curved  
348 relationship (see Equation 4) was observed between the retention of the MXP isomers and  
349 the proportion of MeCN in the mobile phase at pH 6.8 (see Figure 4a for a typical example  
350 on the SuperC18 phase). The use of the standard second order polynomial model (see  
351 Equation 4) used in the retention modelling software was found to generate highly accurate  
352 retention predictions (see retention modelling sections 3.7.1 and 3.7.2).

353

354  $\log k = a + b x$  Equation 3

355

356

357  $\log k = a + b x + c x^2$  Equation 4

358

359 The curved relationship suggested that, at intermediate pH, a mixed mode retention  
360 mechanism was in operation. The negatively charged silanol groups on the phase may  
361 attract the positively charged analytes, via an electrostatic attraction, into the hydrophobic  
362 phase where it can interact with the bonded ligands. A curved relationship (i.e. second  
363 order polynomial model) was also observed at low pH possibly due to a secondary ionic  
364 repulsive interaction (see Figure 4b). In comparison the relationship at pH 10.7 was  
365 observed to be much more linear (see Figure 4c) due to the fact that the MXP isomers were  
366 chromatographed in their ion suppressed form and hence a simple hydrophobic retention  
367 mechanism dominated.

368

369

370

371 3.5 Effect of temperature at intermediate pH

372 If a simple hydrophobic retention mechanism was in operation at pH 6.8, then as the  
373 temperature was increased the retention time should decrease (i.e. van't Hoff relationship)  
374 as shown in Equation 5.

375

$$376 \log k = a + \frac{b}{T} \quad \text{Equation 5}$$

377 Where T = temperature

378

379 However, if the retention is dependent on multiple interactions, then non-linear responses  
380 may be generated and Equation 6 should be more appropriate [18, 21, 22].

381

$$382 \log k = a + \frac{b}{T} + \frac{c}{T^2} \quad \text{Equation 6}$$

383

384 As can be seen in Figure 5, the retention of each MXP isomer on the ACE C18-AR phase  
385 behaved differently as a function of temperature in 10 mM ammonium acetate (pH 6.8)  
386 MeCN/water (54:46 v/v). The 2-MXP isomer exhibited the expected reduction in retention  
387 as temperature increased whereas temperature had little effect on the retention of the 3-  
388 MXP and 4-MXP isomers. These observations may reflect differential changes in the  $pK_a$  of  
389 the MXP isomers and the silanol groups on the stationary phase surface and the pH of the  
390 organic / aqueous mobile phase as temperature is changed and hence the degree of  
391 electrostatic interaction of the regioisomers with the ionized silanol groups. Therefore, it  
392 was inferred that the mechanism controlling the retention and separation of the MXP  
393 regioisomers at pH 6.8 was attributed to an electrostatic interaction which facilitated  
394 hydrophobic interactions.

395

396

397 3.6 Retention behaviour conclusions

398 Stationary phase chemistry appears to have minimal influence on the chromatographic  
399 selectivity of the three MXP regioisomers at low, intermediate or high pH mobile phase  
400 conditions. At low pH mobile phase conditions, the analytes exhibited minimal retention as  
401 a result of mutual repulsion of the adsorbed positively charged analyte on the low acidity  
402 stationary phases. In comparison, at intermediate pH enhanced retention and separation of  
403 the regioisomers was observed. This was attributed to a synergistic effect of the  
404 electrostatic attraction between the ionized analyte and the silanol groups which attracts  
405 the charged analyte into the lipophilic stationary phase where hydrophobic interactions  
406 could take place. In comparison, at high pH the MXP analytes are chromatographed on the  
407 SPP and TPP SuperC18 or phenyl hexyl phases in their neutral form and hydrophobic  
408 interactions were the major retention mechanism.

409

### 410 3.7 Two-dimensional retention modelling and optimization

411 The chromatographic separation of the three isomers was greater at pH 6.8 than at either  
412 pH 3 or 10.7 (see Figures 2a -c). This was further confirmed in preliminary two-dimensional  
413 (gradient time versus temperature) retention modelling studies using the SPP Super  
414 phenylhexyl and C18 phases, as a function of gradient time (i.e. 5 and 15 minutes) and  
415 temperature (i.e. 30 to 65°C) at pH 3 (gradient range 4.5 - 45% MeCN), 6.8 (36 - 90% MeCN)  
416 and 10.7 (36 - 90% MeCN). Four experimental input runs were used to construct the 2 x 2  
417 models using Equations 3 and 5 in the commercial retention modelling software (see  
418 Supplementary electronic information Figures SEI 3 and 4).

419

#### 420 3.7.1 Selection of the most appropriate retention models

421 From the preliminary two-dimensional retention modelling the following operating  
422 parameters were chosen to perform more detailed one-dimensional modelling studies using  
423 the ACE C18-AR, which was observed to generate sharper MXP peaks, to confirm which  
424 equations would generate the most accurate predictions. A temperature range 30 – 75 °C,  
425 and a gradient time range 3 – 12 minutes were evaluated using an initial to final %MeCN of  
426 36 – 63% MeCN. It was found that there was no need to re-define the dwell volume ( $V_D$ )  
427 using an iterative process as excellent results were obtained with the calculated value of  
428 517  $\mu$ L using a slightly modified USP methodology for determining  $V_D$  [23].

429 Table 1 highlighted that the non-standard Equation 4 which described a curved relationship  
430 between  $\log k$  and % organic generated more accurate retention time predictions ( $\Delta t_R$   
431  $<0.11\%$ ) than ~~that of~~ the standard Equation 3 ( $\Delta t_R <0.45\%$ ) for gradient time modelling.

432 In a similar manner, Table 2 highlighted that the non-standard Equation 6 which described a  
433 curved relationship between  $\log$  retention factor ( $k$ ) and  $1/\text{temperature}$  generated more  
434 accurate retention time predictions ( $\Delta t_R <0.23\%$ ) than ~~that of~~ the standard Equations 5  
435 ( $\Delta t_R <2.19\%$ ) for temperature modelling.

436 The LC simulator software utilizes empirical models to calculate peak widths ( $w_{\text{base}}$ ) as  
437 shown in Equations 7, 8 and 9. Where  $\alpha$  and  $\beta$  terms are fitted to minimize the residual for  
438 the retention time of the front ( $t_{R \text{ front}}$ ) and tail ( $t_{R \text{ tail}}$ ) of the peak.

439

$$440 \quad t_{R \text{ tail}} = (1 - \alpha)t_R \quad \text{Equation 7}$$

$$441 \quad t_{R \text{ front}} = (1 + \beta)t_R \quad \text{Equation 8}$$

$$442 \quad w_{\text{base}} = t_{R \text{ front}} - t_{R \text{ tail}} \quad \text{Equation 9}$$

443

444 It should be noted that Equations 1-9 describe isocratic separations, however, by employing  
445 numerical calculations where the gradients are divided into a large number of isocratic  
446 segments, these equations can be equally applied to gradient separations as described here.

447 From Tables 1 and 2 it can be seen that the commercially employed equations are able to  
448 model and predict the peak width to an acceptable degree with errors of <3% being  
449 observed with the models associated with Equations 4 and 6. As a result of the excellent  
450 retention time and acceptable peak width predictions excellent resolution predictions of  
451 <2% were obtainable when Equations 4 and 6 were employed, see Tables 1 and 2.

452

453

### 454 3.7.2 Gradient time *versus* temperature on the C18-AR at pH 6.8

455 As a result of the one-dimensional investigation (see section 3.7.1) the more complex  
456 Equations 6 and 4 were employed in the two-dimensional temperature and gradient time  
457 modelling. In order to model the non-linear relationships of temperature and gradient time  
458 on retention, described in Equations 6 and 4, sixteen input runs (i.e. 4 x 4) were used in  
459 order to generate high quality data.

460 From the two-dimensional model (see Figure 6), it is possible to iteratively change the  $V_D$  in  
461 order to minimize the predicted versus actual retention time errors for an experimental  
462 condition (gradient = 4.5 minutes and temperature = 30°C, often classed as a calibration  
463 run). However, the model using the determined  $V_D$  of 517  $\mu\text{L}$  was shown to generate  
464 <0.08% error for retention time and was hence not changed.

465 The accuracy of the non-linear 4 x 4 retention model (total of 16 input experiments) was  
466 observed to be excellent. The prediction errors for  $t_R$ , peak width and resolution were <0.5  
467 and <13.7% (most were below 5%), <7.8% respectively (see Table 3 and Figure 6) which is  
468 very good compared to the accepted accuracies of 2, 20 and 20% for  $t_R$ , peak width and  
469 resolution respectively [24, 25].

470 The resolution plot of gradient time versus temperature demonstrated that the  
471 methodology was robust (i.e.  $R_s > 2$ ) within the ranges of gradient time (3 to 12 minutes) and  
472 temperature (30 to 75°C), see Figure 6a.

473 A simplified 3 x 3 retention model (i.e. gradient times of 3, 6 and 9 minutes and  
474 temperatures of 30, 45 and 60°C, total of nine input experiments) which is sufficient to  
475 generate second order polynomial relationships generated results very similar to that seen  
476 in the more complex 4 x 4 model see Table 4.

477 It is interesting to note that if one employed the simple linear 2 x 2 retention modelling  
478 using the linear Equations 3 and 5 in a cut down four input data experiment (i.e. gradient  
479 times of 3 and 12 minutes and temperatures of 30 and 75°C), the retention time, peak  
480 width and resolution were <2.3 and <16.4%, <10.7% respectively which is still impressive  
481 given the substantially smaller number of experimental input runs that are required.

482 Conclusion

483 A detailed investigation into the retention behaviour and separation of the regioisomers of  
484 ~~the~~ methoxphenidine (i.e. 2-MXP, 3-MXP and 4-MXP isomers) has shown that, for this  
485 particular separation, the stationary phase chemistry is not a major selectivity parameter.  
486 At low pH, poor separation and retention of the MXP isomers was observed presumably due  
487 to mutual electrostatic repulsion of the adsorbed protonated analytes. In contrast, at  
488 intermediate pH, enhanced retention and separation of all MXP isomers was obtained, it  
489 appeared that there was a synergistic effect between the electrostatic and partitioning  
490 mechanisms. At high pH, the MXP isomers were retained by a predominantly hydrophobic  
491 mechanism due to their unionized form. It was observed that more complicated models  
492 were necessary to fully describe the retention of the MXP isomers due to the fact that  
493 multiple retention mechanisms were in operation. Using these non-linear models with 4 x 4  
494 or 3 x 3 input runs, it was possible to predict with a high degree of certainty (<0.5%) the  
495 retention behaviour of the MXP isomers and then to optimize the gradient separation of the  
496 MXP isomers using a gradient and temperature design space. Prediction errors for peak  
497 width and resolution were in most cases lower than 5%. If one wishes to slightly sacrifice  
498 the prediction accuracy in favour of using a reduced number of experimental input runs,  
499 the linear models using a 2 x 2 model still generated retention time accuracy <2.3% yielding  
500 resolution accuracies of <11%.

501 Subsequently, from the 4 x 4 retention model, a rapid and highly sensitive LC-MS friendly  
502 method (i.e.  $R_{s \text{ min}} > 3$  within 2.5 minutes) was predicted and verified. The developed  
503 methodology should be highly suitable for the rapid, specific and sensitive detection and  
504 control of these novel illicit drugs within bulk forensic samples.

505

506 Conflict of interest

507 The authors have declared no conflict of interest.

508

509 Acknowledgements

510 The authors are grateful to the following: The Chromatographic Society for support through  
511 a summer studentship to B. Boateng; L. Steel and J. Field, Strathclyde Institute of Pharmacy  
512 and Biomedical Sciences (SIPBS) for performing the early column screening work and non-  
513 linear work respectively; Advanced Chemistry Development for providing the LC simulator  
514 and physical / chemical properties software and Advanced Chromatography Technologies  
515 for providing the columns used in this work.

516

517

518 References

- 519 [1] L. A. King, Legal Classification of Novel Psychoactive Substances: An International  
520 Comparison, In Novel Psychoactive Substances, edited by P.I. Dargan, D.M. Wood,  
521 Academic Press, Boston, (2013), Chapter 1, 3-27, ISBN 9780124158160,  
522 <http://dx.doi.org/10.1016/B978-0-12-415816-0.00001-8>.
- 523 [2] S.W. Smith, F.M. Garlich, Availability and Supply of Novel Psychoactive Substances, In  
524 Novel Psychoactive Substances, edited by P.I. Dargan, D.M. Wood, Academic Press,  
525 Boston, (2013), Chapter 3, 55-77, ISBN 9780124158160,  
526 <http://dx.doi.org/10.1016/B978-0-12-415816-0.00003-1>.
- 527 [3] M.C. Van Hout, E.Hearne, "Word of Mouse": Indigenous Harm Reduction and Online  
528 Consumerism of the Synthetic Compound Methoxphenidine, J. Psychoactive Drugs,  
529 47 (2015) 30-41.
- 530 [4] L.A. King, A.T. Kicman, A brief history of 'new psychoactive substances', Drug Test.  
531 Anal., 3 (2011) 401–403.
- 532 [5] J. Wallach, P.V. Kavanagh, G. McLaughlin, N. Morris, J.D. Power, S.P. Elliot, M.S.  
533 Mercier, D. Lodge, H. Morris, N.M. Dempster, S.D. Brandt, Preparation and  
534 characterisation of the "research chemical" diphenidine, its pyrrolidine analogue,  
535 and their 2,2-diphenylethyl isomers, Drug Test Anal. 7(5) (2015) 358-267.
- 536 [6] G. McLaughlin, N. Morris, P.V. Kavanagh, J.D. Power, J. O'Brien, B. Talbot, S.P. Elliott,  
537 J. Wallach, K. Hoang, H. Morris, S.D. Brandt, Test purchase, synthesis, and  
538 characterization of 2-methoxydiphenidine (MXP) and differentiation from its meta -  
539 and para -substituted isomers. Drug Test Anal., 8 (2016) 98-109.  
540 <http://doi.org/10.1002/dta.1800>
- 541 [7] H. Morris, J. Wallach, From PCP to MXE: a comprehensive review of the non-medical  
542 use of dissociative drugs, Drug Test Anal. 6(7-8) (2016) 614-632.
- 543 [8] P. Reuter, B. Pardo, Can new psychoactive substances be regulated effectively? An  
544 assessment of the British Psychoactive Substances Bill, Addiction 112 (1) (2017) 25-  
545 31.
- 546 [9] A. Helander, O. Beck, M. Baeckberg, Intoxications by the dissociative new  
547 psychoactive substance diphenidine and methoxphenidine, Clin Toxicol 53(5) (2015)  
548 446-453.
- 549 [10] S.P. Elliot, S.D. Brandt, J. Wallach, H. Morris, P.V. Kavanagh, First reported fatalities  
550 associated with the "research chemical" 2-methoxydiphenidine, J Anal Toxicol 39(4)  
551 (2015) 287-293.

552

553

- 554 [11] P.M. Geyer, M.C. Hulme, J.P.B. Irving, P.D. Thompson, R.N. Ashton, R.J. Lee, L.  
555 Johnson, J. Marron, C.E. Banks and O.B. Sutcliffe, Guilty by Dissociation –  
556 Development of Gas Chromatography-Mass Spectrometry (GC-MS) and other rapid  
557 screening methods for the analysis of 13 diphenidine- derived New Psychoactive  
558 Substances (NPSs), *Anal Bioanal Chem*, 408 (29) (2016) 8467-8481.
- 559 [12] M.R. Euerby, M. Fever, J. Hulse, M. James, P. Petersson, C. Pipe, Maximization of  
560 Selectivity in Reverse Phase Liquid Chromatographic Method Development  
561 Strategies, *LC•GC Europe*, 29 (2016) 8 – 21.
- 562 [13] <http://www.ace-hplc.com/technical-area/literature.aspx#2733>. Accessed 3<sup>rd</sup> May  
563 2016.
- 564 [14] M.R. Euerby, P. Petersson, Chromatographic classification and comparison of  
565 commercially available reversed-phase liquid chromatographic columns using  
566 principal component analysis, *J. Chromatogr. A* 994 (2003) 13-36.
- 567 [15] M.R. Euerby, P. Petersson, W. Campbell, W. Roe, Chromatographic classification and  
568 comparison of commercially available reversed-phase liquid chromatographic  
569 columns containing phenyl moieties using principal component analysis, *J.*  
570 *Chromatogr. A* 1154 (2007) 138-151.
- 571 [16] P. Jandera, M. Janderov, J. Churcek, Gradient elution in liquid chromatography: VIII.  
572 Selection of the optimal composition of the mobile phase in liquid chromatography  
573 under isocratic conditions, *J Chromatogr. A* 148 (1978) 79-97.
- 574 [17] Y. Baba, G. Kura, Computer-assisted retention prediction system for inorganic cyclic  
575 polyphosphates and its application to optimization of gradients in anion-exchange  
576 chromatography, *J Chromatogr. A* 550 (1991) 5-14.
- 577 [18] M.R. Euerby, J. Hulse, P. Petersson, A. Vazhentsev, K. Kassam, Retention Modelling in  
578 Hydrophilic Interaction Chromatography, *Anal Bioanal Chem* 40 (2015) 9135-9152.
- 579 [19] L.R. Snyder, J.W. Dolan, J.R. Gant, Gradient elution in high-performance liquid  
580 chromatography : I. Theoretical basis for reversed-phase systems, *J Chromatogr. A*  
581 165 (1979) 3-30.
- 582 [20] P. Jandera, J. Churcek, L. Svoboda, Gradient elution in liquid chromatography: X.  
583 Retention characteristics in reversed-phase gradient elution chromatography, *J*  
584 *Chromatogr. A* 174 (1979) 35-50.
- 585 [21] P. Petersson, J. Munch, M.R. Euerby, A. Vazhentsev, M. McBrien, S.K. Bhal, K.  
586 Kassam, Adaption of Retention Models to Allow Optimisation of Peptide and Protein  
587 Separations. *Chromatography Today* 7 (2007) 15-18.
- 588 [22] T. Galaon, V. David, Deviation from van't Hoff dependence in RP-LC induced by  
589 tautomeric interconversion observed for four compounds, *J Sep Sci* 34 (2011) 1423-  
590 1428.

591 [23] Chromatographic system suitability tests signal to noise USP 37 <621>  
592 <https://hmc.usp.org/sites/default/files/documents/HMC/GCs-Pdfs/c621.pdf>.  
593 Accessed 19th December 2016

594 [24] R.G. Wolcott, J.W. Dolan, L.R. Snyder, Computer simulation for the convenient  
595 optimization of isocratic reversed-phase liquid chromatographic separations by  
596 varying temperature and mobile phase strength, *J Chromatogr. A* 869 (2000) 3-25,

597 [25] L.R. Snyder, J.W. Dolan, *High-Performance Gradient Elution: The Practical Application*  
598 *of the Linear-Solvent-Strength Model*, Hoboken, NJ: Wiley, (2007) pp. 399.

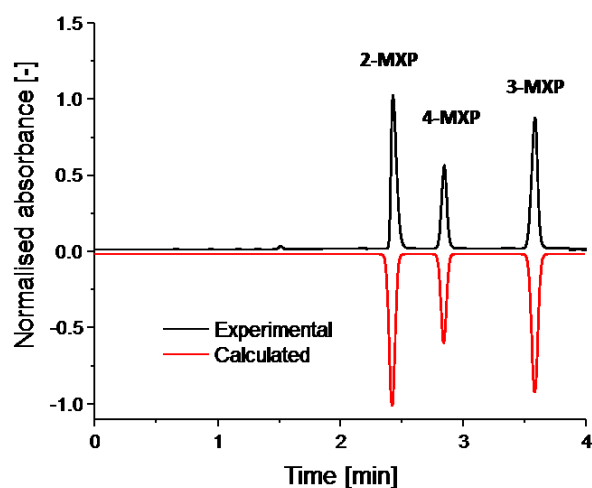
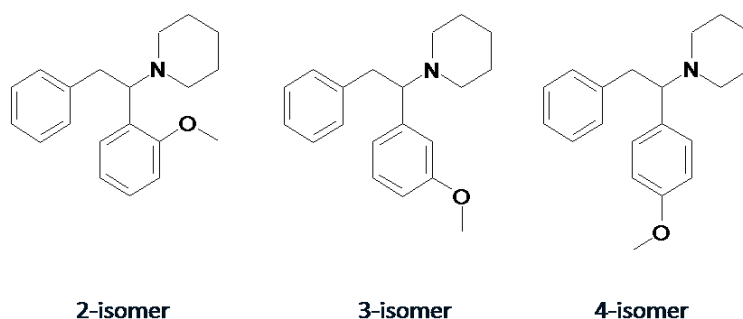
599  
600  
601  
602

603 Highlights

- 604 • Retention / separation of MXP regioisomers is controlled by electrostatic /  
605 hydrophobic mechanisms
- 606 • Non-linear models were generated to describe the effect of % organic and  
607 temperature on retention
- 608 • Two-dimensional (gradient time versus temperature) modelling was highly accurate
- 609 • Rapid separation of MXP regioisomers was achieved by retention modelling and  
610 optimization
- 611 • A rapid / highly sensitive LC-MS method ( $R_{s \text{ min}} > 3$  within 2.5 minutes) was predicted  
612 and verified

613

614 Graphical highlight



615

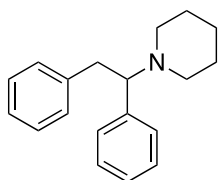
616

617

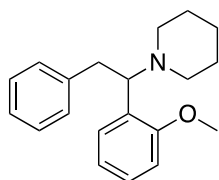
618 Figure 1. Structure of the diphenidine (1) and methoxydiphenidine regioisomers (2, 2-  
619 MXP; 3, 3-MXP and 4, 4-MXP).

620

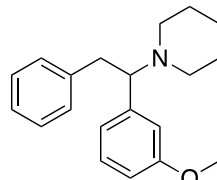
621



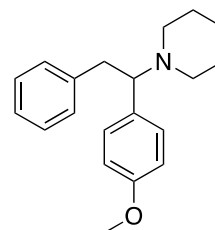
622 Diphenidine (1)



623 2-Methoxyphenidine  
(2, 2-MXP)



624 3-Methoxyphenidine  
(3, 3-MXP)



4-Methoxyphenidine  
(4, 4-MXP)

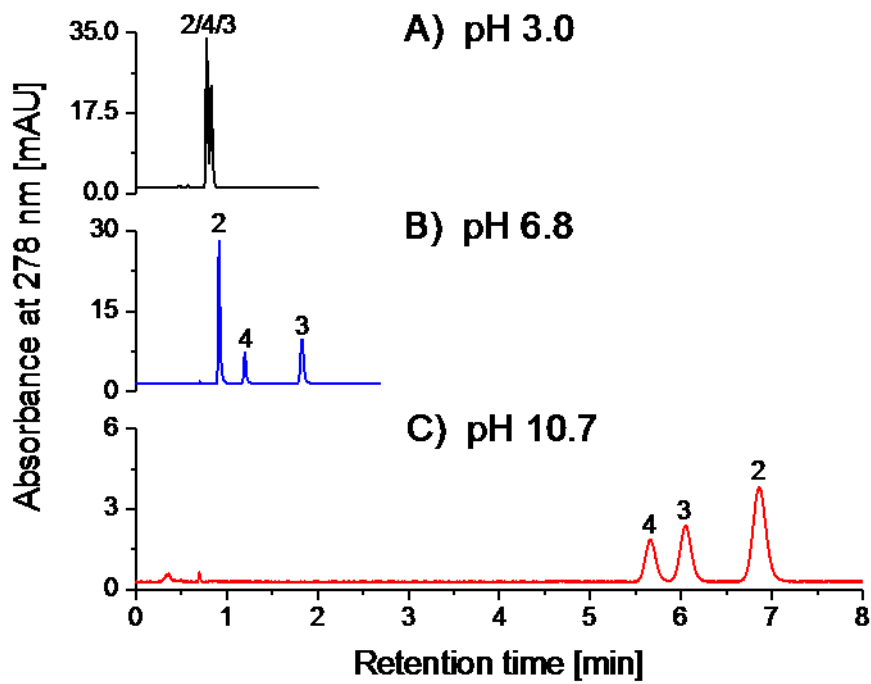
623

624

625

626 Figure 2

627 Separation of the MXP isomers (2-, 3- and 4-isomers) on an ACE UltraCore  
628 SuperC18 2.5  $\mu\text{m}$  50 x 4.6 mm column, 50  $^{\circ}\text{C}$ , 1 mL  $\text{min}^{-1}$ , Agilent 1290 Infinity  
629 Quaternary UHPLC, mobile phase of MeCN : water (54:46 v/v) containing a)  
630 10 mM ammonium formate pH 3, b) 10 mM ammonium acetate (unadjusted  
631 pH of 6.8) and c) 18 mM ammonia (unadjusted pH of 10.7). MXP isomer  
632 assignment as shown in the chromatograms.



633

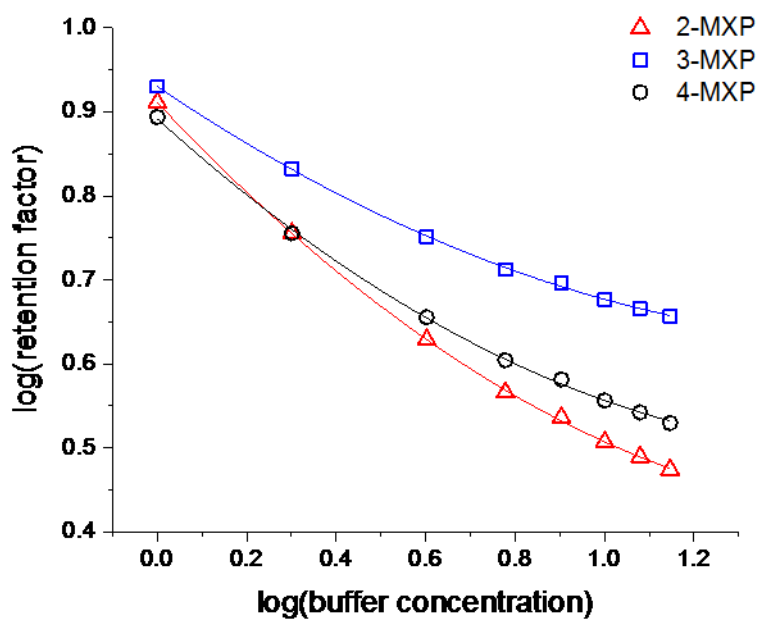
634

635

636

637 Figure 3. Effect of buffer concentration on the retention on the regioisomers at pH 6.8  
638 using an ACE C18-AR, 3  $\mu\text{m}$ , 50 x 4.6 mm column, ammonium acetate (pH 6.8)  
639 in MeCN/water (54:46 v/v), 30  $^{\circ}\text{C}$ , 1 mL  $\text{min}^{-1}$ , Agilent 1290 Infinity  
640 quaternary UHPLC.

641



642

643

644 Figure 4. The effect of the proportion of MeCN, on the retention of the MXP  
645 isomers performed on an ACE SuperC18 3  $\mu\text{m}$  50 x 4.6 mm column, 1  
646  $\text{mL min}^{-1}$ , 60  $^{\circ}\text{C}$ , Agilent 1290 Infinity binary UHPLC. Mobile phase A  
647 buffer in water, mobile phase B buffer in MeCN/water (9:1 v/v).

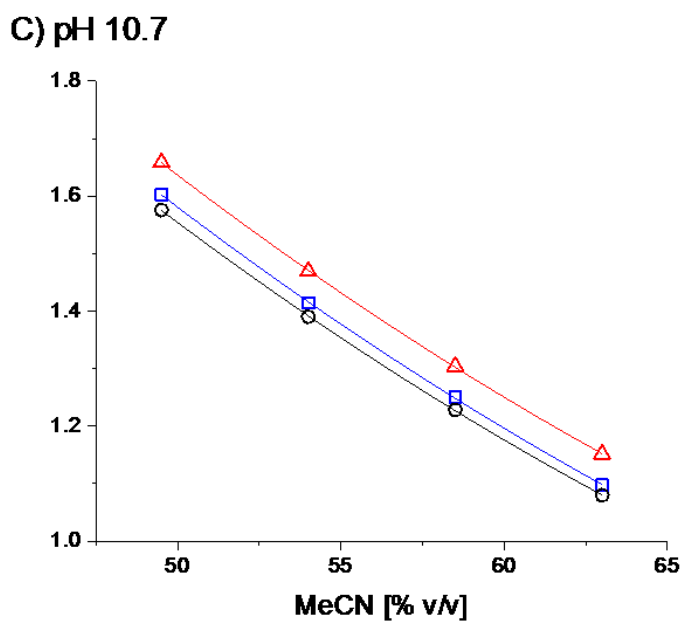
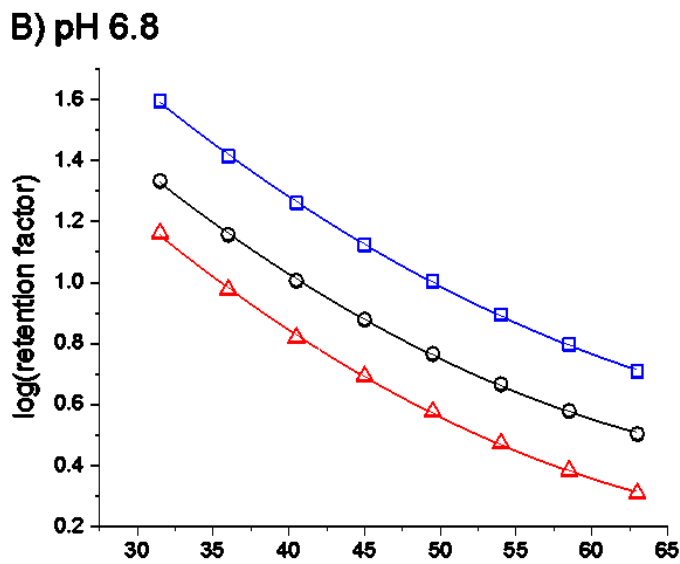
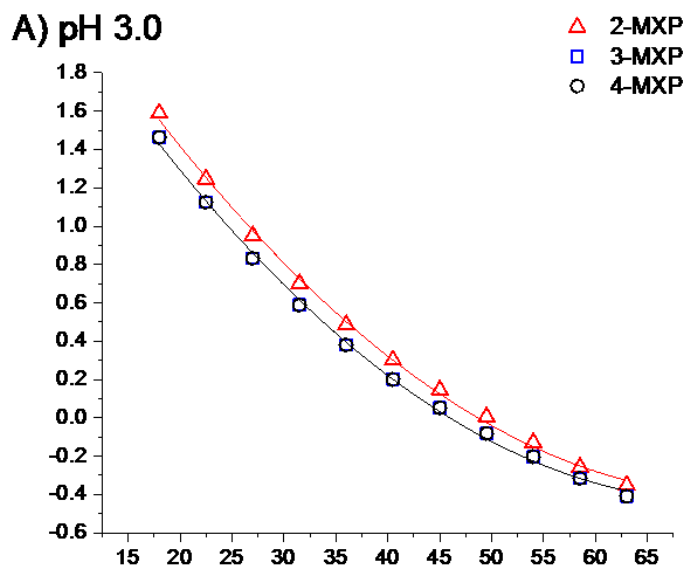
648

649 4a) buffer 10 mM ammonium formate (pH 3.0).

650 4b) buffer 10 mM ammonium acetate (pH 6.8 unadjusted).

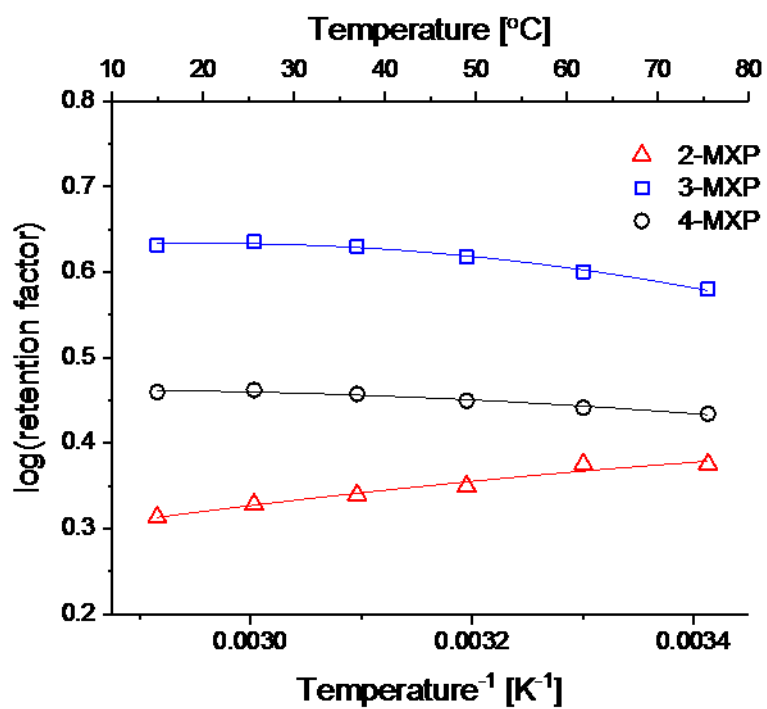
651 4c) buffer 18.6 mM ammonia (pH 10.7).

652



655 Figure 5. The effect of 1/temperature ( $^{\circ}\text{K}$ ) on the log of the retention factor of the MXP  
656 isomers performed on an ACE C18-AR 3  $\mu\text{m}$  50 x 4.6 mm column using 10 mM  
657 ammonium acetate (pH 6.8 unadjusted) in MeCN/water 54:46 v/v, 1 mL  $\text{min}^{-1}$   
658 using the Shimadzu Nexera X2 UHPLC.

659



660

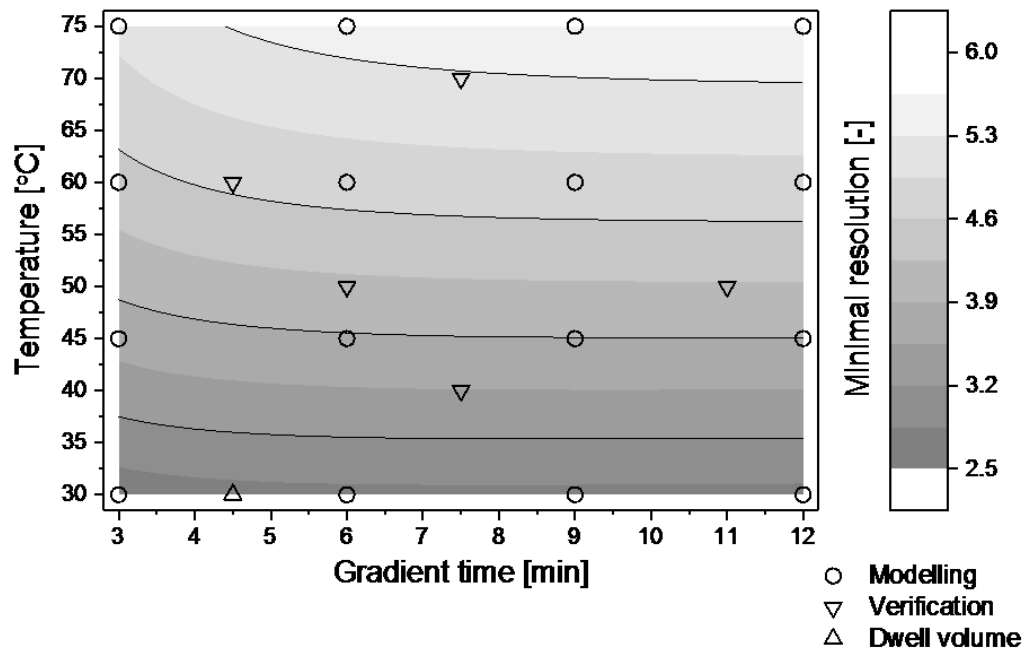
661

662 Figure 6. a) Two-dimensional retention model (gradient time versus temperature) for  
 663 the ACE C18-AR, 3  $\mu\text{m}$ , 50 x 4.6 mm column, 1 mL min<sup>-1</sup>, mobile phase A) 10  
 664 mM ammonium acetate (pH 6.8 unadjusted) in water and B) 10 mM  
 665 ammonium acetate (pH 6.8 unadjusted) in MeCN/water (9:1 v/v), gradient 40  
 666 to 70%B, Nexera X2 UHPLC with a V<sub>D</sub> and V<sub>m</sub> of 517 and 458  $\mu\text{L}$  respectively.  
 667 b) Experimental and predicted chromatograms performed with a gradient  
 668 and temperature of 4.5 min and 60 °C.

669

670

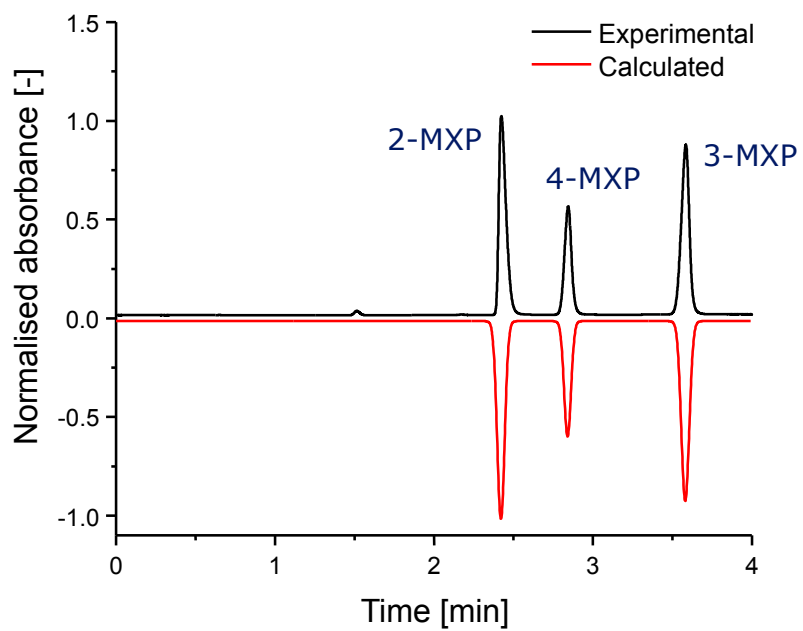
Figure 6a



671

672

673



675

676

677

678 Table 1. Prediction errors for gradient time models using Equations 3 (gradient inputs of 3  
 679 and 12 min) and 4 (gradient inputs of 3, 6, 9 and 12 min) as assessed by an interpolation of  
 680 the retention at a gradient time of 4.5 minutes using a temperature of 30°C, where % $\Delta$   
 681 retention time ( $t_R$ ) = (predicted  $t_R$  – actual  $t_R$ )/ actual  $t_R$ , % $\Delta$  peak width at 4 x standard  
 682 deviation ( $4\sigma$ ) = (predicted peak width at  $4\sigma$  – actual peak width at  $4\sigma$ )/ actual peak width at  
 683  $4\sigma$ , % $\Delta$   $R_s$  at  $4\sigma$  = (predicted resolution ( $R_s$ ) at  $4\sigma$  – actual  $R_s$  at  $4\sigma$ )/ actual  $R_s$  at  $4\sigma$ .  $V_D$  and the  
 684 column void volume ( $V_m$ ) = 517 and 458  $\mu$ L respectively.

685

Equation 3		Predicted			Actual			$\Delta t_R$ (min)		$\Delta$ width (min)		$\Delta R_s$ (USP)		Model used
Peak Name	$t_R$ (min)	Width (min)	$R_s$ (USP)	$t_R$ (min)	Width (min)	$R_s$ (USP)	$\Delta t_R$ (min)	% $\Delta t_R$	$\Delta$ width (min)	% $\Delta$ width	$\Delta R_s$ (USP)	% $\Delta R_s$ (USP)		
2-MXP	2.486	0.108		2.477	0.109		0.009	0.36	-0.001	-0.65			a = 4.9666, b = -7.8663e-2, c = 0.0000	
4-MXP	2.729	0.088	2.48	2.72	0.087	2.49	0.009	0.33	0.001	1.59	-0.01	-0.34	a = 4.8601, b = -7.2282e-2, c = 0.0000	
3-MXP	3.378	0.096	7.05	3.363	0.099	6.95	0.015	0.45	-0.003	-2.55	0.11	1.56	a = 5.0037, b = -6.6316e-2, c = 0.0000	

686

Equation 4		Predicted			Actual			$\Delta t_R$ (min)		$\Delta$ width (min)		$\Delta R_s$ (USP)		Model used
Peak Name	$t_R$ (min)	Width (min)	$R_s$ (USP)	$t_R$ (min)	Width (min)	$R_s$ (USP)	$\Delta t_R$ (min)	% $\Delta t_R$	$\Delta$ width (min)	% $\Delta$ width	$\Delta R_s$ (USP)	% $\Delta R_s$ (USP)		
2-MXP	2.475	0.110		2.477	0.109		-0.002	-0.08	0.001	1.19			a = 7.7101, b = -1.9844e-1, c = 1.2937e-3	
4-MXP	2.717	0.088	2.44	2.720	0.087	2.49	-0.003	-0.11	0.001	1.59	-0.04	-1.75	a = 7.0448, b = -1.6585e-1, c = 9.8928e-4	
3-MXP	3.361	0.100	6.85	3.363	0.099	6.95	-0.002	-0.06	0.001	1.51	-0.10	-1.37	a = 6.7427, b = -1.3715e-1, c = 7.0815e-4	

687

688

689 Table 2. Accuracy of the temperature models using Equations 5 (temperature inputs of 30  
 690 and 70°C) and 6 (temperature inputs of 30, 45, 60 and 70°C) as assessed by an interpolation  
 691 of the retention at 50°C using a gradient time of 6 minutes where % $\Delta t_R$  = (predicted  $t_R$  –  
 692 actual  $t_R$ )/ actual  $t_R$ , % $\Delta$  peak width at  $4\sigma$  = (predicted peak width at  $4\sigma$  – actual peak width  
 693 at  $4\sigma$ )/ actual peak width at  $4\sigma$ , % $\Delta R_s$  at  $4\sigma$  = (predicted  $R_s$  at  $4\sigma$  – actual  $R_s$  at  $4\sigma$ )/ actual  $R_s$   
 694 at  $4\sigma$ .  $V_D$  and  $V_m$  = 517 and 458  $\mu$ L respectively.

695

Equation 5		Predicted			Actual			$\Delta t_R$ (min)		$\Delta$ width (min)		$\Delta R_s$ (USP)		Model
Peak	$t_R$ (min)	Width (min)	$R_s$ (USP)	$t_R$ (min)	Width (min)	$R_s$ (USP)	$\Delta t_R$ (min)	% $\Delta t_R$	$\Delta$ width (min)	% $\Delta$ width	$\Delta R_s$ (USP)	% $\Delta R_s$ (USP)		
2-MXP	2.547	0.106		2.574	0.100		-0.027	-1.05	0.006	5.78			a = 1.1179, b = 1.2912e+2	
4-MXP	2.947	0.097	3.94	2.988	0.093	4.28	-0.041	-1.37	0.004	3.83	-0.34	-7.84	a = 2.1439, b = -1.4570e+2	
3-MXP	3.747	0.112	7.66	3.831	0.109	8.34	-0.084	-2.19	0.003	3.03	-0.69	-8.22	a = 2.5724, b = -1.9410e+2	

696

Equation 6		Predicted			Actual			$\Delta t_R$ (min)		$\Delta$ width (min)		$\Delta R_s$ (USP)		Model
Peak	$t_R$ (min)	Width (min)	$R_s$ (USP)	$t_R$ (min)	Width (min)	$R_s$ (USP)	$\Delta t_R$ (min)	% $\Delta t_R$	$\Delta$ width (min)	% $\Delta$ width	$\Delta R_s$ (USP)	% $\Delta R_s$ (USP)		
2-MXP	2.568	0.103		2.574	0.100		-0.006	-0.23	0.003	2.78			a = -9.8483e-1, b = 1.4981e+3, c = -2.2174e+5	
4-MXP	2.985	0.095	4.21	2.988	0.093	4.28	-0.003	-0.10	0.002	1.69	-0.06	-1.50	a = -1.0249, b = 1.9168e+3, c = -3.3403e+5	
3-MXP	3.829	0.111	8.19	3.831	0.109	8.34	-0.002	-0.05	0.002	2.11	-0.15	-1.77	a = -2.5816, b = 3.1609e+3, c = -5.4338e+5	

697

698 Table 3. Predicted, actual and accuracy of retention time, peak width and resolution from  
 699 the two-dimensional models (see Figure 6) using equation 4 ( $t_G$  inputs of 3, 6, 9 and 12 min)  
 700 and equation 6 (temperature inputs of 30, 45, 60 and 70°C) as assessed by five interpolation  
 701 conditions within the design space, where  $\% \Delta t_R = (\text{predicted } t_R - \text{actual } t_R) / \text{actual } t_R$ ,  $\% \Delta$   
 702 peak width at  $4\sigma = (\text{predicted peak width at } 4\sigma - \text{actual peak width at } 4\sigma) / \text{actual peak}$   
 703 width at  $4\sigma$ ,  $\% \Delta R_s \text{ at } 4\sigma = (\text{predicted } R_s \text{ at } 4\sigma - \text{actual } R_s \text{ at } 4\sigma) / \text{actual } R_s \text{ at } 4\sigma$ .  $V_D$  and  $V_m =$   
 704 517 and 458  $\mu\text{L}$  respectively.

705

Peak	Temperature (°C) $t_G$ (min)		Predicted			Actual								
			$t_R$ (min)	Width (min)	$R_s$ (USP)	$t_R$ (min)	Width (min)	$R_s$ (USP)	$\Delta t_R$ (min)	$\% \Delta t_R$	$\Delta$ width (min)	$\% \Delta$ width	$\Delta R_s$ (USP)	$\% \Delta R_s$ (USP)
2-MXP	70	7.5	2.585	0.111		2.576	0.098		0.010	0.37	0.013	13.27		
4-MXP			3.151	0.105	5.24	3.145	0.103	5.67	0.006	0.19	0.002	1.94	-0.43	-7.52
3-MXP			4.121	0.126	8.40	4.117	0.124	8.56	0.005	0.11	0.002	1.61	-0.16	-1.88
Peak	50	6	$t_R$ (min)	Width (min)	$R_s$ (USP)	$t_R$ (min)	Width (min)	$R_s$ (USP)	$\Delta t_R$ (min)	$\% \Delta t_R$	$\Delta$ width (min)	$\% \Delta$ width	$\Delta R_s$ (USP)	$\% \Delta R_s$ (USP)
2-MXP			2.566	0.104		2.574	0.100		-0.008	-0.31	0.004	4.00		
4-MXP			2.982	0.095	4.18	2.988	0.093	4.30	-0.006	-0.20	0.002	2.15	-0.12	-2.77
3-MXP	3.827	0.113	8.13	3.831	0.109	8.30	-0.004	-0.10	0.004	3.67	-0.18	-2.11		
Peak	50	11	Predicted			Actual								
			$t_R$ (min)	Width (min)	$R_s$ (USP)	$t_R$ (min)	Width (min)	$R_s$ (USP)	$\Delta t_R$ (min)	$\% \Delta t_R$	$\Delta$ width (min)	$\% \Delta$ width	$\Delta R_s$ (USP)	$\% \Delta R_s$ (USP)
2-MXP			2.793	0.124		2.792	0.123		0.001	0.04	0.002	1.22		
4-MXP	3.303	0.117	4.23	3.302	0.115	4.29	0.002	0.05	0.002	1.74	-0.06	-1.36		
3-MXP	4.415	0.146	8.46	4.411	0.144	8.58	0.004	0.09	0.003	1.74	-0.13	-1.49		
Peak	60	4.5	Predicted			Actual								
			$t_R$ (min)	Width (min)	$R_s$ (USP)	$t_R$ (min)	Width (min)	$R_s$ (USP)	$\Delta t_R$ (min)	$\% \Delta t_R$	$\Delta$ width (min)	$\% \Delta$ width	$\Delta R_s$ (USP)	$\% \Delta R_s$ (USP)
2-MXP			2.420	0.094		2.423	0.085		-0.003	-0.12	0.009	10.59		
4-MXP	2.840	0.086	4.67	2.843	0.083	5.00	-0.003	-0.11	0.003	3.61	-0.33	-6.67		
3-MXP	3.580	0.099	8.00	3.584	0.095	8.32	-0.003	-0.10	0.004	4.21	-0.32	-3.85		
Peak	40	7.5	Predicted			Actual								
			$t_R$ (min)	Width (min)	$R_s$ (USP)	$t_R$ (min)	Width (min)	$R_s$ (USP)	$\Delta t_R$ (min)	$\% \Delta t_R$	$\Delta$ width (min)	$\% \Delta$ width	$\Delta R_s$ (USP)	$\% \Delta R_s$ (USP)
2-MXP			2.680	0.112		2.672	0.117		0.009	0.32	-0.005	-4.27		
4-MXP	3.059	0.102	3.54	3.047	0.102	3.43	0.013	0.41	0.000	0.49	0.11	3.19		
3-MXP	3.955	0.122	8.00	3.940	0.122	7.99	0.016	0.39	0.000	0.00	0.01	0.11		

706

707

708 Table 4. Predicted, actual and accuracy of retention time, peak width and resolution from  
 709 the two-dimensional models using equation 4 ( $t_G$  inputs of 3, 6 and 9 min) and equation 6  
 710 (temperature inputs of 30, 45 and 60°C) as assessed by three interpolation conditions within  
 711 the design space, where  $\% \Delta t_R = (\text{predicted } t_R - \text{actual } t_R) / \text{actual } t_R$ ,  $\% \Delta \text{ peak width at } 4\sigma =$   
 712  $(\text{predicted peak width at } 4\sigma - \text{actual peak width at } 4\sigma) / \text{actual peak width at } 4\sigma$ ,  $\% \Delta R_s \text{ at } 4\sigma =$   
 713  $(\text{predicted } R_s \text{ at } 4\sigma - \text{actual } R_s \text{ at } 4\sigma) / \text{actual } R_s \text{ at } 4\sigma$ .  $V_D$  and  $V_m = 517$  and  $458 \mu\text{L}$   
 714 respectively.

715

Peak	Temperature (°C) $t_G$ (min)		Predicted			Actual			$\Delta t_R$ (min) $\% \Delta t_R$		$\Delta \text{ width (min) } \% \Delta \text{ width}$		$\Delta R_s$ (USP) $\% \Delta R_s$ (USP)	
	50	6	$t_R$ (min)	Width (min)	$R_s$ (USP)	$t_R$ (min)	Width (min)	$R_s$ (USP)	$\Delta t_R$ (min)	$\% \Delta t_R$	$\Delta \text{ width (min)}$	$\% \Delta \text{ width}$	$\Delta R_s$ (USP)	$\% \Delta R_s$ (USP)
2-MXP	50	6	2.567	0.107		2.574	0.100		-0.008	-0.31	0.004	4.00		
4-MXP			2.984	0.096	4.11	2.988	0.093	4.30	-0.006	-0.20	0.002	2.15	-0.19	-4.46
3-MXP			3.828	0.113	8.08	3.831	0.109	8.30	-0.004	-0.10	0.004	3.67	-0.22	-2.69
	60	4.5	Predicted			Actual			$\Delta t_R$ (min) $\% \Delta t_R$		$\Delta \text{ width (min) } \% \Delta \text{ width}$		$\Delta R_s$ (USP) $\% \Delta R_s$ (USP)	
Peak			$t_R$ (min)	Width (min)	$R_s$ (USP)	$t_R$ (min)	Width (min)	$R_s$ (USP)	$\Delta t_R$ (min)	$\% \Delta t_R$	$\Delta \text{ width (min)}$	$\% \Delta \text{ width}$	$\Delta R_s$ (USP)	$\% \Delta R_s$ (USP)
2-MXP			2.422	0.096		2.423	0.085		-0.003	-0.12	0.009	10.59		
4-MXP	2.841	0.086	4.60	2.843	0.083	5.00	-0.003	-0.11	0.003	3.61	-0.40	-7.91		
3-MXP	3.581	0.099	8.00	3.584	0.095	8.32	-0.003	-0.10	0.004	4.21	-0.32	-3.85		
	40	7.5	Predicted			Actual			$\Delta t_R$ (min) $\% \Delta t_R$		$\Delta \text{ width (min) } \% \Delta \text{ width}$		$\Delta R_s$ (USP) $\% \Delta R_s$ (USP)	
Peak			$t_R$ (min)	Width (min)	$R_s$ (USP)	$t_R$ (min)	Width (min)	$R_s$ (USP)	$\Delta t_R$ (min)	$\% \Delta t_R$	$\Delta \text{ width (min)}$	$\% \Delta \text{ width}$	$\Delta R_s$ (USP)	$\% \Delta R_s$ (USP)
2-MXP			2.679	0.115		2.672	0.117		0.009	0.32	-0.005	-4.27		
4-MXP	3.059	0.102	3.50	3.047	0.102	3.43	0.013	0.41	0.000	0.49	0.07	2.03		
3-MXP	3.955	0.123	7.96	3.940	0.122	7.99	0.016	0.39	0.000	0.00	-0.03	-0.33		

716